Shock effects in plagioclase feldspar from the Mistastin Lake impact structure, Canada

Annemarie E. Pickersgill[1*†], Gordon R. Osinski[1, 2], and Roberta L. Flemming[1]
[1]Dept. of Earth Sciences and Centre for Planetary Science and Exploration, University of Western Ontario, 1151 Richmond St., London, Ontario, N6A 5B7, Canada
[2]Dept. of Physics and Astronomy, The University of Western Ontario, 1151 Richmond St., London, Ontario, N6A 5B7, Canada

[*] Corresponding author. E-mail: a.pickersgill.1@research.gla.ac.uk
[†] Current address: School of Geographical & Earth Sciences, University of Glasgow, Gregory Building, Lilybank Gardens, Glasgow G12 8QQ, U.K.

Abstract – Shock metamorphism, caused by hypervelocity impact, is a poorly understood process in feldspar due to the complexity of the crystal structure, the relative ease of weathering, and chemical variations, making optical studies of shocked feldspars challenging. Understanding shock metamorphism in feldspars, and plagioclase in particular, is vital for understanding the history of Earth's moon, Mars, and many other planetary bodies. We present here a comprehensive study of shock effects in andesine and labradorite from the Mistastin Lake impact structure, Labrador, Canada. Samples from a range of different settings were studied, from in situ central uplift materials to clasts from various breccias and impact melt rocks. Evidence of shock metamorphism includes undulose extinction, offset twins, kinked twins, alternate twin deformation, and partial to complete transformation to diaplectic plagioclase glass. In some cases, isotropization of alternating twin lamellae was observed. Planar deformation features (PDFs) are notably absent in the plagioclase, even when present in neighboring quartz grains. It is notable that various microlites, twin planes, and compositionally different lamellae could easily be mistaken for PDFs and so care must be taken. A pseudomorphous zeolite phase (levyne-Ca) was identified as a replacement mineral of diaplectic feldspar glass in some samples, which could, in some instances, also be potentially mistaken for PDFs. We suggest that the lack of PDFs in plagioclase could be due to a combination of structural controls relating to the crystal structure of different feldspars and/or the presence of existing planes of weakness in the form of twin and cleavage planes.

INTRODUCTION

Meteorite impact craters are a dominant surface feature on most terrestrial planetary bodies. The temperatures and pressures that result from crater-forming hypervelocity impacts are well above those observed in endogenic geologic processes, the results of which include solid-state deformation of lithic and mineral fragments, termed shock metamorphic effects (see e.g., French and Koeberl 2010, Ferrière and Osinski 2013, and references therein). Evidence of shock metamorphism includes diagnostic shock effects such as planar deformation features (PDFs) and diaplectic glasses, which are exclusive to impact, and features such as undulose extinction, fracturing, and optical mosaicism, which are not exclusive to hypervelocity impact as they can also be formed during endogenic processes, but which are none-the-less indicative of non-uniform strain caused by the passage of the shockwave.

The terms *diaplectic feldspar glass* and *maskelynite* are often used interchangeably; however, observations interpreted as evidence of flow in some meteoritic maskelynite (e.g., Chen and El Goresy 2000), and poorly defined usage of the term over the past century, has made universal understanding of the definition of maskelynite ambiguous. When maskelynite was first described, it was interpreted as an unknown, isotropic mineral of near labradorite composition (Tschermak 1872), and later as a monomineralic glass of near labradorite composition (Tschermak 1883). It was Binns (1967), who first suggested that it had a shock origin. Since then, the meaning of the term maskelynite has become ambiguous, therefore, we do not use the term maskelynite in reference to our study. Instead, we refer to monomineralic shock-amorphized material, which shows no signs of flow, as diaplectic feldspar glass (Chao 1967; Engelhardt and Stöffler 1968).

Thus far, studies of shock effects in feldspar group minerals have been limited due to the optical complexity of the crystal structure and the comparatively rapid rate at which feldspars weather, making them difficult to study using conventional optical techniques. As a result, feldspar is often ignored in favor of quartz for use as a shock indicator and barometer. This has resulted in a limited, purely qualitative, shock scale for feldspar (see Table 1) (e.g., Stöffler 1966; Lambert 1979; Ostertag and Jessberger 1982; Ostertag 1983; Stöffler et al. 1991), despite some studies having suggested that feldspar can be just as useful as quartz (e.g., Kayama et al. 2012; Jaret et al. 2014). An understanding of shock effects in feldspars is vital for planetary studies, which often deal with quartz-poor, but feldspar-rich, lithologies, including terrestrial anorthosites and basalts (e.g., Wolfe 1972, Kieffer et al. 1976, Schaal and Hörz 1977).

The aim of this study is to investigate solid state shock effects in plagioclase feldspar, motivated by the dominance of plagioclase in the anorthositic lunar highlands. This contribution will address solid state shock-related deformation of plagioclase feldspars at the Mistastin Lake impact structure, Labrador, Canada, an excellent lunar analogue site with anorthosite target rocks. This forms part of a larger project that is aimed at developing a more quantitative scale of shock deformation in feldspar group minerals and thereby expanding the utility of feldspar for determining shock level in quartz-limited systems (e.g., anorthosite, many mafic rocks, and meteorites); and for determining which technique(s) are the most effective in evaluating shock deformation in feldspars

GEOLOGICAL SETTING

The Mistastin Lake impact structure, known locally as Kamestastin, located in central Labrador, Canada (55°53'N; 63°18'W), is comprised of an oval-shaped lake located in a large depression that is enclosed by an approximately 28 km diameter ring of hills – generally regarded as being the remnant crater rim (Grieve 2006). There is an island near the centre of the lake, which is interpreted as being the central uplift of the complex crater structure. Topographic similarities to other impact structures suggested a meteorite impact origin (Taylor and Dence 1969), which was subsequently confirmed by the discovery of shock metamorphosed rocks and minerals including quartz and feldspar exhibiting planar deformation features (PDFs), diaplectic quartz and feldspar glasses, and poorly developed shatter cones (Taylor and Dence 1969). Whole rock isotopic age dating techniques using $^{40}Ar/^{39}Ar$ methods and the decay constants of Steiger and Jäger (1977), have given the Mistastin Lake impact structure an age of 36 ± 4 Ma (Mak et al. 1976). A more recent age determination yielded a CA TIMS U/Pb zircon age of 37.83 ± 0.05 Ma (Sylvester et al. 2013). Dating of zircon from Mistastin using the low-temperature (U-Th)/He technique yielded a preferred apparent age of 32.7 ± 1.2 Ma (Young et al. 2013).

The Mistastin Lake impact structure is located within the Mistastin Lake batholith, a part of the Canadian shield, composed of three main lithologies: anorthosite, granodiorite, and a pyroxene-rich quartz monzonite (sometimes called mangerite) (Fig. 1) (Currie 1971; Emslie and Stirling 1993). Taylor and Dence (1969) reported strong irregular fracturing in all minerals and the development of several sets of planar features in quartz and feldspar. In feldspars, Taylor and Dence (1969) noted the local development of 1 to 3 sets of planar features and slight to moderate hydrothermal alteration that has affected the feldspars after passage of the shockwave.

METHODS AND SAMPLES

Samples of shocked feldspar-bearing lithologies were collected over the course of three field seasons from a range of locations throughout the Mistastin structure (Fig. 1, Table 2) – with the intent of obtaining a wide range of shock levels and, therefore, a diverse sampling of shock metamorphic effects. The majority of samples in this study come from anorthosite target rock or monomict anorthosite breccia; some additional samples are individual mineral clasts in polymict lithic and melt-bearing breccias, and some are from the granodiorite or monzonite that make up the remainder of the three main types of target rock.

Polished thin sections were examined for microscopic shock metamorphic features, using a Nikon Eclipse LV100POL compound petrographic microscope. Follow up work on microtextures was conducted with backscattered electron (BSE) imagery using a Zeiss 1540XB FIB/SEM at the Nanofabrication Laboratory at The University of Western Ontario. Quantitative chemical composition and cathodoluminescence data were collected using a JXA-8530F Field Emission Electron Probe Microanalyzer (FE-EPMA) in the Earth and Planetary Materials Analysis Laboratory at The University of Western Ontario. Beam operating conditions were an accelerating voltage of 10 kV-15 kV, probe current of 20 nA, and a beam diameter of <5 µm. Mineral calibration standards used for wavelength dispersive spectrometry (WDS) analyses were as follows: albite (CM Taylor) for Na and Si, orthoclase (CM Taylor) for Si and K, and anorthite (Smithsonian USNM 137041 - Great Sitkin Island, AL) for Al and Ca.

Mineral identification by micro-X-ray diffraction was performed in the Department of Earth Sciences at The University of Western Ontario on a Bruker D8 Discover diffractometer with theta-theta instrument geometry as described by Flemming (2007). It has a sealed cobalt

source (CoKα: λ = 1.8789 Å), Gobel mirror parallel beam optics, a pinhole collimator (100 or 300 μm), and two-dimensional (2-D) general area detector diffraction system (GADDS). Omega scans were used, wherein the source and detector rotate simultaneously, both clockwise, through a specified number of degrees (the Omega angle, °ω) to simulate rotation of the sample. Counting time was 30 minutes for GADDS frame 1 (θ_1=14.5°, θ_2=16°, ω=6°) and 45 minutes for GADDS frame 2 (θ_1=30°, θ_2=40°, ω=23°). Observed lattice planes were indexed using ICDD cards: 01-079-1148 (C)-andesine, 01-083-1417 (C)-labradorite, and 00-046-1263 (C)-levyne-Ca.

RESULTS

Anorthosite samples are dominated by plagioclase feldspar, often altered along fractures to zeolites and clay minerals, with minor amounts of quartz, pyroxene, and sulfides. Ubiquitous small dark rod-like microlites are present along cleavage and twin planes within plagioclase grains (Fig. 2). These microlites were too small to obtain fully quantitative EPMA or μXRD analyses due to beam overlap with surrounding phases. Nevertheless, analyses of their chemical composition revealed increased Fe content relative to the surrounding feldspar, up to 100 wt% in some cases, with additional Ti and trace Mg. We have, therefore, tentatively identified them as being of the ilmenite-hematite solid solution of iron-oxides. They match in composition, habit, and orientation the microlites reported in clouded feldspars (e.g., Poldervaart and Gilkey 1954; Whitney 1972). Clouding is thought to occur by exsolution or diffusion of iron post-formation (e.g., Poldervaart and Gilkey 1954; Whitney 1972), and is therefore not considered to be related to shock processes. Granodiorite and monzonite samples are also dominated by plagioclase feldspar. Additional minerals present in these samples include potassium feldspar, pyroxene, quartz, diverse alteration products, and sulfides. All mineral grains in each lithology are heavily fractured and exhibit undulose extinction. In all three lithologies, plagioclase crystals are large (mm-size or greater), well formed, and exhibit well-developed polysynthetic twinning. Individual plagioclase mineral clasts are common in impact breccias throughout the crater and as clasts in the impact melt rocks. The various solid-state shock effects and shock-induced deformations observed in plagioclase grains from Mistastin Lake are reported in the next sections. A summary of the geographic distribution of observed shock features can be found in Table 2.

Deformed twins and fracturing

Curved and kinked twins were observed in several plagioclase samples from around the crater. Kinked twins resemble kink banding in micas in that they turn sharply away from normal linear twins (Figs. 3A, B). Evidence of this kinking is only visible in cross-polarized light. In plane polarized light, the crystals appear unstrained. Twins that are bent in a smoother curve are more common, and the angle through which they bend can vary significantly from less than 1° up to ~25° (Figs. 3C, D). Varying degrees of undulose extinction are exhibited by feldspar grains from throughout the crater. Often the degree of undulose extinction varies even in neighboring grains in the same thin section.

Fractures are ubiquitous and tend to be relatively long but are not planar. They cross crystal boundaries and are often steeply angled to twin planes. Alteration to clays and zeolites tends to be concentrated along fractures. Increased alteration around fractures to clay minerals and zeolites indicates that these fractures pre-existed sample collection and preparation. Whether

or not the fractures resulted from formation of the impact crater or as a result of normal terrestrial processes is unknown. Some twins are offset up to 30 µm by micro-faults (fractures which have resulted in movement of one side of the mineral grain relative to the other). Samples from outside the central uplift are notably less fractured than those from the central uplift. Planar fractures (PFs) in plagioclase were not observed.

Planar Elements

Undecorated planar deformation features (PDFs) were observed in *all* quartz grains in thin sections from the central uplift (Fig. 4A). Interestingly, quartz from outside the central uplift contains only decorated PDFs or, more commonly, no PDFs at all. One of the most unexpected results of this study is that *no* PDFs were observed in feldspar grains of any composition, at any location in the crater. Some features in anorthosite from the central uplift, observed in transmitted light, superficially resemble PDFs restricted to alternate twin lamellae (Fig. 4B). They are approximately perpendicular to twin planes, and abruptly change orientation further up the length of the twins to become oblique to twin planes (Fig. 4B). However, upon closer inspection, it is apparent that these features are actually thin lenses that possess a different composition than the host mineral (Fig. 4C, D). This differentiates the observed features from PDFs, which are amorphous lamellae of the same composition and consistent thickness across the length (French and Koeberl 2010). The Fe-oxide microlites mentioned above can also be mistakenly identified as planar deformation features on cursory examination (Fig. 2). However, on close inspection (at high optical magnification or with BSE imaging), they show themselves to be acicular rather than planar, to be discontinuous throughout the crystal, to remain birefringent under cross-polarized light when present in isotropic grains (diaplectic feldspar glasses), and to be of non-feldspathic composition.

Diaplectic Glass

All diaplectic feldspar glasses discussed here meet the following three criteria (as suggested by French and Koeberl (2010)): 1) identification of grains as isotropic and pseudomorphous to plagioclase; 2) composition that matches monomineralic plagioclase feldspar as seen by EPMA; and 3) an amorphous state as confirmed by µXRD. No diaplectic quartz glasses were observed.

Partial Isotropization

Several grains appear to have been only partially converted to diaplectic glass. This is evident in that in a crystal that appears cohesive in plane polarized light, part will remain extinct on rotation of the stage in cross-polarized light, while the rest of the crystal remains birefringent (Fig. 5). In many of these grains, there do not appear to be any crystallographic restrictions on which part has become amorphous (Fig. 5). There are several cases, however, in which the partial isotropization of plagioclase grains does appear to be crystallographically controlled, manifesting in the isotropization of only alternate twin lamellae (Fig. 6). EPMA analyses of these twins showed no appreciable change in the composition between crystalline and diaplectic glass (isotropic) twins (Table 3).

Complete Isotropization

More common than partial isotropization is the complete conversion of feldspar grains to diaplectic glass. In several thin sections, all of the feldspar has become isotropic. The chemical composition is homogenous over various beam spots and grains in these sections (Table 3). In plane polarized light, isotropic grains are clear and do not appear any more altered or differently fractured than the crystalline plagioclase of other samples from the same area (Fig. 7A). Under cross-polarized light, these grains are completely isotropic (Fig. 7B) (i.e., they remain extinct on rotation) and they produce amorphous patterns (akin to extreme peak broadening resulting in total erasure of individual peaks) when examined with μXRD. Like much of the plagioclase throughout anorthosite samples at Mistastin, the isotropic grains appear to include many Fe-oxide microlites. The microlites are all aligned in the same direction, and do not appear to have been disrupted. They match the morphology and optical properties of similar microlites in crystalline feldspathic grains from other samples.

One clast of diaplectic glass in a polymict impact breccia shows lamellar features with the appearance of relict twins in plane polarized light (Fig. 8). The surface of that grain was examined using secondary electron imaging, and no surficial artefacts were observed that would explain them. This grain was also imaged using cathodoluminescence (CL) and BSE imaging, but no trace of the lamellae was found. CL images of some other diaplectic glass grains showed possible evidence of remnant twins (Fig. 7D). These linear features are slightly less luminescent than the surrounding crystal. They are faint, narrow, and line up with the microlites visible in the photomicrographs. Unlike the Fe-oxide microlites, they are continuous across the grain and they are not visible in the BSE images (Fig. 7C).

Alteration

An unusual extinction pattern was observed first in anorthosite samples from the central uplift, and, subsequently, in clasts and in the matrix of brecciated target rocks from South Creek (see Fig. 1 for locations). When rotated under cross-polarized light, these grains show a mottled pseudo-fibrous radial extinction pattern similar to that described as plumose by McIntyre (1968) (Fig. 9). In one sample, this pattern has a more vein-like texture in places cross-cutting crystal boundaries (Figs. 9A, B), but in other places stopping abruptly at crystal boundaries, or restricted to alternate twin lamellae (Figs. 9C-F). In other samples, the same pattern is observed as pseudomorphous with entire feldspar clasts, and rimming plagioclase clasts in polymict and monomict impact breccias.

Micro-X-ray diffraction (μXRD) studies show the crystalline structure of the plumose material to be the zeolite levyne-Ca (Fig. 10), known to occur naturally only in cavities of basaltic rocks or synthesized from basaltic glass (Deer et al. 2004). Electron probe microanalysis (EPMA) results (summarized in Table 3) confirm the μXRD findings, through a chemical composition consistent with levyne-Ca (Deer et al. 2004). In the case of the zeolitized twins, it is important to note that the extensions of the zeolitized twins vary in composition compared to the surrounding crystal by less than 1% (Table 3). This indicates that the chemical change is associated with the zeolite only, and not an inherent property of the twins (an observation which is confirmed by chemical composition of the vein-like zeolite).

In plane-polarized light, these zeolites are easily mistaken for plagioclase crystals. They bear every resemblance to clear, unaltered, well-formed plagioclase, often preserving evidence of

twinning and the aligned Fe-oxide microlites present in plagioclase crystals of the surrounding material. In the case in which zeolites are restricted to only alternate twin lamellae, there is a fracture set that is abruptly truncated by the altered twins. The perpendicular fractures exist in the normal twins, next to the unaltered extensions of the zeolitized twins, as well (Fig. 9). There are multiple other instances of alternate twins altering, while their neighbors maintain their original composition and form. In these cases, the alteration is visible as grey-brown darkening of the twins visible in plane-polarized light, and reduced transmission under both plane- and cross-polarized light.

DISCUSSION

Planar Elements

Many of the petrographic observations in our study corroborate those of earlier studies at Mistastin Lake, including the presence of pervasive irregular fracturing throughout minerals, lateral displacement along fractures (offset twins, etc.), and planar deformation features in quartz (Taylor and Dence 1969). However, in contrast to the findings of Taylor and Dence (1969), no planar deformation features were found in plagioclase anywhere in the crater structure. In several instances, the discovery of planar deformation features was thought to have occurred but on closer inspection, these textures turned out to be zeolitization along pre-existing crystal planes (Fig. 4), or faint clouding (Fe-oxide microlites) in plagioclase grains (Fig. 2).

French and Koeberl (2010) report from references therein that PDFs in quartz and feldspar form at approximately the same pressures (~10–30 GPa). In this study, samples from the central uplift invariably showed well-developed, undecorated planar deformation features in quartz grains (Fig. 4A,B), while the feldspar showed none at all. The presence of PDFs in quartz in these sections, coupled with their absence in neighboring plagioclase, is, therefore, surprising, and implies one or more of the following explanations: 1) PDFs form in plagioclase much less readily than in quartz and than previously thought; and/or 2) that PDFs in feldspars are more difficult to recognize than in quartz due to coincidence with pre-existing planar features such as cleavage and twin planes; and/or 3) that PDFs are more easily erased in plagioclase than in quartz. The pristine nature of PDFs in quartz grains (Fig. 4) suggests that these samples have not been affected by annealing or any major post-impact alteration. Therefore, it seems unlikely that alteration or annealing could account for the lack of PDFs in feldspars.

Does composition play a role? The chemical composition of PDF-containing feldspars is often not reported, but when compositional data have been provided, the feldspars are more often of the low-Ca ($An_{<30}$) plagioclase or K-feldspar series rather than Ca-rich plagioclase (Trepmann et al. 2003; Gibson and Reimold 2005; Nagy et al. 2008). The plagioclase at Mistastin is An_{31-55}. This may imply that there is a structural/compositional control that encourages PDF development in the Ca-poor plagioclase and alkali series over the Ca-rich plagioclases. The plagioclase series is consistently triclinic ($>An_{10}$), the albite end-member can be monoclinic (at >980°C) (Deer et al. 2001). In the alkali series, anorthoclase is also triclinic at room temperature, but can be monoclinic at crystallization temperatures, and sanidine is always monoclinic (Deer et al. 2001). We hypothesize that the higher symmetry of monoclinic feldspars may encourage formation of PDFs in Ca-poor plagioclase and potassium feldspars over Ca-rich plagioclases. Other crystal systems in which PDFs have been reported include: monoclinic (diopside), orthorhombic (sillimanite, cordierite, olivine, orthopyroxene), isometric (garnet),

hexagonal (apatite, quartz), and tetragonal (zircon) (e.g., Dworak 1969; Stöffler 1972, 1974; Stöffler et al. 1991; Dressler 1990; Bohor et al. 1993; Nesse 2004; Wittmann et al. 2006). Our study shows that it is imperative, then, that the chemical composition is reported for studies of feldspars, as the shock effects seem to vary significantly with chemical composition.

A further possible explanation for the lack of PDFs or planar fractures (PFs) in plagioclase feldspar could be related to pre-existing planes of weakness (e.g., twin planes, cleavage) in plagioclase, which may allow "relief" of pressure caused by passage of the shockwave, and that this mechanism of pressure release precludes – or greatly inhibits – the formation of PDFs. This does not necessarily mean that plagioclase feldspars can never form PDFs, only that they are far less common than perhaps originally reported (cf., Gibbons and Ahrens 1977), and that they likely form under a much narrower range of pressure conditions, as is supported by Ostertag (1983) particularly in labradorite.

Diaplectic Glass

In diaplectic plagioclase glasses (e.g., Fig. 7), the remnants of pre-existing structure are still visible, through the arrangement of the Fe-oxide microlites. Crystallographically controlled alignment of Fe-oxide microlites, the possible preservation of twins, and the preservation of outward crystal boundaries (Figs. 7, 8) support the interpretation that these glasses formed as the result of a solid-state transition between crystalline and amorphous material. This evidence precludes the possibility of low-viscosity melting, as microlites would certainly be disrupted in all but the most viscous, and temporary of melts. It supports a lack of flow, which has been suggested to occur in meteoritic maskelynite (Chen and El Goresy 2000), calling on the surrounding crystals to contain the apparent mineral melt, resulting in a glass which seems to have maintained an external crystal form. In the samples involved in this study, no glasses were found that appeared to be the result of highly viscous melts, as one might expect as a transitional state between diaplectic and natural melt glasses, however, as this study focused on solid-state effects, samples more likely to contain melt phases were largely excluded from the work.

The preferential shock deformation of only alternate twin lamellae has been discussed previously by Stöffler (1966), Short and Gold (1996), and Gibson and Reimold (2005). Our observations of diaplectic glass forming in only alternate twin lamellae support these observations and support the hypothesis that the orientation of the shockwave relative to the orientation of the crystal affects the degree and type of shock deformation that occur (Stöffler 1966).

Alteration

Zeolitization, in this case, is interpreted to be the result of preferential low-temperature hydrothermal alteration of a shock-weakened plagioclase structure to levyne-Ca. The selective formation of levyne-Ca in only alternate twins is reminiscent of the way in which diaplectic feldspar glass occasionally occurs. A possible explanation for this is that the twins previously converted to diaplectic feldspar glass are preferentially altering to zeolites and not the remaining crystalline twins. Metastable feldspathic glass, produced through melting or solid state amorphization would be particularly susceptible to alteration to a zeolite. This hypothesis matches the reported synthesis of levyne-Ca from basaltic glass (Wirsching 1981), the pseudomorphous shock vitrification of plagioclase, and the observation of alternate twin lamellae

becoming isotropic, as a result of shock. Therefore, it seems probable that much of the zeolitization observed in these samples is the result of secondary processes enabled by shock metamorphism. No circumstance, other than shock metamorphism, as far as we are aware, results in deformation of only alternate twin lamellae.

Sieve-textured or "checkerboard" plagioclase

Sieve-textured or "checkerboard" plagioclase has been previously been reported at Mistastin Lake by Grieve (1975), but was not observed in this work. Grieve (1975) found this texture in inclusions of unshocked plagioclase in a fine-to-medium-grained clast-poor impact melt rock, and described it as partially digested inclusions in which the rectangular digested domains are filled by melt products (Grieve 1975). Bischoff and Stöffler (1984) found sieve-textured feldspars in a similar setting from the Lappajärvi crater, Finland, and concluded that "checkerboard" feldspar clasts are the result of crystallization of feldspar subgrains above the solidus, and not the result of a subsolidus reaction. Thus, the lack of sieve-textured or "checkerboard" plagioclase is not too surprising given the majority of our samples are from various breccias and the central uplift and not from impact melt rocks (Table 2).

CONCLUDING REMARKS

The most widely recognized diagnostic shock metamorphic feature in plagioclase feldspars at Mistastin is diaplectic feldspar glass. Inferences about the degree of shock can be made based on the degree to which single crystals have been isotropized (the entire crystal, part of the crystal, only alternate twins, etc.). Because diaplectic glasses lose more internal structure with increasing shock level (e.g., Lambert and Grieve 1984), it appears that at higher pressures twins become less evident and the degree of chemical homogenization increases – as diaplectic glasses get closer to being monomineralic melt glasses. Other features, such as fracturing and undulose extinction, can be indicative of shock metamorphism but are definitely not diagnostic.

Further investigation into the nature of planar deformation features in plagioclase needs to involve the investigation of twin and cleavage planes by finer scale techniques to identify if glass is present along those planes, indicative of PDFs, as in quartz, parallel to rational crystallographic planes but masked by coincident pre-existing planar features in the mineral. We also encourage all workers to report the chemical composition of the feldspars studied in order to investigate the potential role of this parameter in PDF formation.

Acknowledgements – the Natural Sciences and Engineering Research Council of Canada, the Northern Scientific Training Program, and the Canadian Space Agency are thanked for the generous funding they provided. Marianne Mader, Cassandra Marion, Marc Beauchamp, Alaura Singleton and Rodney Dammeier are thanked for their support in the field and sharing samples from previous field seasons. The Nanofabrication Facility at the University of Western Ontario is thanked for funding and training for using their SEM. The Earth and Planetary Materials Analysis (EPMA) Laboratory, also at Western, is gratefully acknowledged for the EPMA work. Martin Schmieder and Ludovic Ferrière are thanked for their helpful and thorough reviews of this paper.

REFERENCES

Binns R. A. 1967. Stony meteorites bearing maskelynite. *Nature* 213: 1111–1112.

Bohor B. F., Betterton W. J., and Krogh T. E. 1993. Impact-shocked zircons: discovery of shock-induced textures reflecting increasing degrees of shock metamorphism. *Earth and Planetary Science Letters* 119: 419–424.

Chao E. C. T. 1967. Impact Metamorphism. *Researches in Geochemistry,* 2: 204–233.

Chen M., and El Goresy A. 2000. The nature of maskelynite in shocked meteorites; not diaplectic glass but a glass quenched from shock-induced dense melt at high pressures. *Earth and Planetary Science Letters* 179: 489–502.

Currie K. L. 1971. Geology of the resurgent cryptoexplosion crater at Mistastin Lake, Labrador. *Bulletin - Geological Survey of Canada 207*. 62 p.

Deer W. A., Howie R. A., and Zussman J. 2001. *Rock-forming minerals, volume 4A: framework silicates - feldspars*, 2nd ed. London: The Geological Society. 972 p.

Deer W. A., Howie R. A., Wise W. S., and Zussman J. 2004. *Rock-forming minerals, volume 4B: framework silicates - silica minerals, feldspathoids and zeolites*, 2nd ed. London: The Geological Society. 982 p.

Dressler B. 1990. Shock metamorphic features and their zoning and orientation in the Precambrian rocks of the Manicouagan Structure, Quebec, Canada. *Tectonophysics* 171: 229–245.

Dworak U. 1969. Stoßwellenmetamorphose des Anorthosits vom Manicouagan Krater, Quebec, Canada. *Contributions to Mineralogy and Petrology* 24: 306–347.

Emslie R. F., and Stirling J. A. R. 1993. Rapakivi and related granitoids of the Nain plutonic suite: geochemistry, mineral assemblages and fluid equilibria. *The Canadian Mineralogist* 31: 821–847.

Engelhardt W. von, and Stöffler D. 1968. Stages of shock metamorphism in crystalline rocks of the Ries Basin, Germany. In *Shock metamorphism of natural materials*, edited by French B. M., and Short N. M. Baltimore, MD: Mono Book Corp. pp. 159–168.

Ferrière, L., Osinski, G.R., 2013. Shock metamorphism. In: Osinski, G.R., Pierazzo, E. (Eds.), Impact Cratering: Processes and Products, first ed. Wiley-Blackwell, New Jersey, pp. 106–124 (Chapter 8).

Flemming R. L. 2007. Micro X-ray Diffraction (μXRD): A versatile technique for characterization of Earth and planetary materials. *Canadian Journal of Earth Sciences* 44: 1333–1346.

French B. M., and Koeberl C. 2010. The convincing identification of terrestrial meteorite impact structures: What works, what doesn't, and why. *Earth-Science Reviews* 98: 123–170.

Gibbons R. V. and Ahrens T. J. 1977. Effects of Shock Pressures on Calcic Plagioclase. *Physics and Chemistry of Minerals* 1: 95–107

Gibson R. L., and Reimold W. U. 2005. Shock pressure distribution in the Vredefort impact structure, South Africa. *Geological Society of America Special Paper* 384: 329–349.

Grieve R. A. F. 1975. Petrology and chemistry of the impact melt at Mistastin Lake crater, Labrador. *Geological Society of America Bulletin* 86: 1617–1629.

Grieve R. A. F. 2006. *Impact structures in Canada*, St. John's, N.L.: Geological Association of Canada. 210 p.

Jaret S., Kah L. C., and Harris R. S. 2014. Progressive deformation of feldspar recording low-barometry impact processes, Tenoumer impact structure, Mauritania. *Meteoritics and Planetary Science* 49(6):1007-1022.

Kayama M., Nishido H., Sekine T., Nakazato T., Gucsik A., and Ninagawa K. 2012. Shock barometer using cathodoluminescence of alkali feldspar. *Journal of Geophysical Research* 117: E09004.

Kieffer S. W., Schaal R. B., Gibbons R., Hörz F., Milton D. J., Dube A. 1976. Shocked basalt from Lonar Impact Crater, India, and experimental analogues. *Proceedings of the Lunar Science Conference*. 7: 1391-1412.

Lambert P. 1979. Fractures induced by shock in quartz and feldspar. *Mineralogical Magazine* 43: 527–533.

Lambert P., and Grieve R. A. F. 1984. Shock experiments on maskelynite-bearing anorthosite. *Earth and Planetary Science Letters* 68: 159–171.

Mader M. M. and Osinski G. R. 2011. Insight into lunar impact cratering processes based on field mapping of the Mistastin Lake Impact Structure, Labrador (abstract #P43C-1698). *American Geophysical Union Fall Meeting Abstracts*.

Mader M. M., Osinski G. R., and Tornabene L. L. 2013. Structural geology of the Mistastin Lake impact structure, Labrador, Canada (abstract #2517). *44th Lunar and Planetary Science Conference*.

Mader M. M. and Osinski G. R. 2013b. Impact melt-bearing breccias of the Mistastin Lake impact structure: A unique planetary analogue for ground-truthing proximal ejecta emplacement (abstract #P34C-01). *American Geophysical Union Fall Meeting Abstracts*.

Mak E., York D., Grieve R. A. F., and Dence M. 1976. The age of the Mistastin Lake crater, Labrador, Canada. *Earth and Planetary Science Letters* 31: 345–357.

Marion C. L., and Sylvester P. J. 2010. Composition and heterogeneity of anorthositic impact melt at Mistastin Lake crater, Labrador. *Planetary and Space Science* 58: 552–573.

McIntyre D. B. 1968. Impact Metamorphism at Clearwater Lake, Quebec. In *Shock metamorphism of natural materials*, edited by French B. M., and Short N. M. Baltimore: Mono Book Corp. pp. 363–366.

Nagy S., Gucsik A., Bérczi S., Ninagawa K., Nishido H., Kereszturi A., Hargitai H., and Okumura T. 2008. K-feldspar and biotite as shock indicator minerals from Bosumtwi impact crater (abstract #1144). *39th Lunar and Planetary Science Conference*.

Nesse W. D. 2004. *Introduction to optical mineralogy*, 3rd ed. New York: Oxford University Press. 348 p.

Ostertag R. 1983. Shock experiments on feldspar crystals. *Journal of Geophysical Research* 88, Suppl.: B364–B376.

Ostertag R., and Jessberger E. K. 1982. Shock-effects on the K-Ar system of plagioclase feldspar and the age of anorthosite inclusions from North-Eastern Minnesota. *Geochimica et Cosmochimica Acta* 46: 1465–1471.

Poldervaart A., and Gilkey A. K. 1954. On clouded plagioclase. *American Mineralogist* 35: 75–91.

Schaal R. B. and Hörz F. 1977. Shock metamorphism of lunar and terrestrial basalts. *Proceedings of the Lunar Science Conference*. 8: 1697–1729.

Short N. M., and Gold D. P. 1996. Petrography of shocked rocks from the central peak at the Manson impact structure. *Geological Society of America Special Paper* 302: 245–265.

Singleton A. C., Osinski G. R., McCausland P. J. A., and Moser D. E. 2011. Shock-induced changes in density and porosity in shock-metamorphosed crystalline rocks, Haughton impact structure, Canada. *Meteoritics & Planetary Science* 46: 1774–1786.

Steiger R. H., and Jäger E. 1977. Subcommission on geochronology: convention on the use of decay constants in geo- and cosmochronology. *Earth and Planetary Science Letters* 36: 359–362.

Stöffler D. 1966. Zones of impact metamorphism in the crystalline rocks of the Nördlinger Ries crater. *Contributions to Mineralogy and Petrology* 12: 15–24.

Stöffler D. 1971. Progressive metamorphism and classification of shocked and brecciated crystalline rocks at impact craters. *Journal of Geophysical Research* 76: 5541–5551.

Stöffler D. 1972. Deformation and transformation of rock-forming minerals by natural and experimental shock processes: I. Behavior of minerals under shock compression. *Fortschritte der Mineralogie* 49: 50–113.

Stöffler D. 1974. Deformation and transformation of rock-forming minerals by natural and experimental shock processes: II. Physical properties of shocked minerals. *Fortschritte der Mineralogie* 51: 256–289.

Stöffler D., Keil K., and Scott E. R. D. 1991. Shock metamorphism of ordinary chondrites. *Geochimica et Cosmochimica Acta* 55: 3845–3867.

Sylvester P. J., Crowley J. L., and Schmitz M. D. 2013. U/Pb zircon age of Mistastin Lake crater, Labrador, Canada – implications for high-precision dating of small impact melt sheets and the end Eocene extinction. (abstract #5248). *Goldschmidt 2013*.

Taylor F. C., and Dence M. R. 1969. A probable meteorite origin for Mistastin Lake, Labrador. *Canadian Journal of Earth Sciences* 6: 39–45.

Trepmann C., Whitehead J., and Spray J. 2003. Shock effects in target rocks from the Charlevoix impact structure, Quebec, Canada.

Tschermak G. 1872. Die Meteoriten von Shergotty und Gopalpur. *Sitzungsberichte der Mathematisch-Naturwissenschaftlichen Klasse der Kaiserlichen Akademie der Wissenschaften, Wien* 65: 122–145.

Tschermak G. 1883. Beitrag zur Classification der Meteoriten. *Sitzungsberichte der Mathematisch-Naturwissenschaftlichen Klasse der Kaiserlichen Akademie der Wissenschaften, Wien* 88: 347–371.

Whitney P. R. 1972. Spinel inclusions in plagioclase of metagabbros from the Adirondack Highlands. *American Mineralogist* 57: 1429–1436.

Wirsching U. 1981. Experiments on the hydrothermal formation of calcium zeolites. *Clays & Clay Minerals*. 29: 171–183

Wittmann A., Kenkmann T., Schmitt R. T., and Stöffler D. 2006. Shock-metamorphosed zircon in terrestrial impact craters. *Meteoritics & Planetary Science* 41: 433–454.

Wolfe S. H. 1972. Part I. Geology of the Manicouagan-Mushalagan Lakes Structure. Part II. Geochronology of the Manicouagan-Mushalgan Lakes Structure. *PhD Thesis*, Caltech, 473p.

Young K. E., Hodges K. V, van Soest M. C., and Osinski G. R. 2013. Dating the Mistastin Lake impact structure, Labrador, Canada, using zircon (U-Th)/He thermochronology (abstract #2426). *44th Lunar and Planetary Science Conference*.

FIGURES

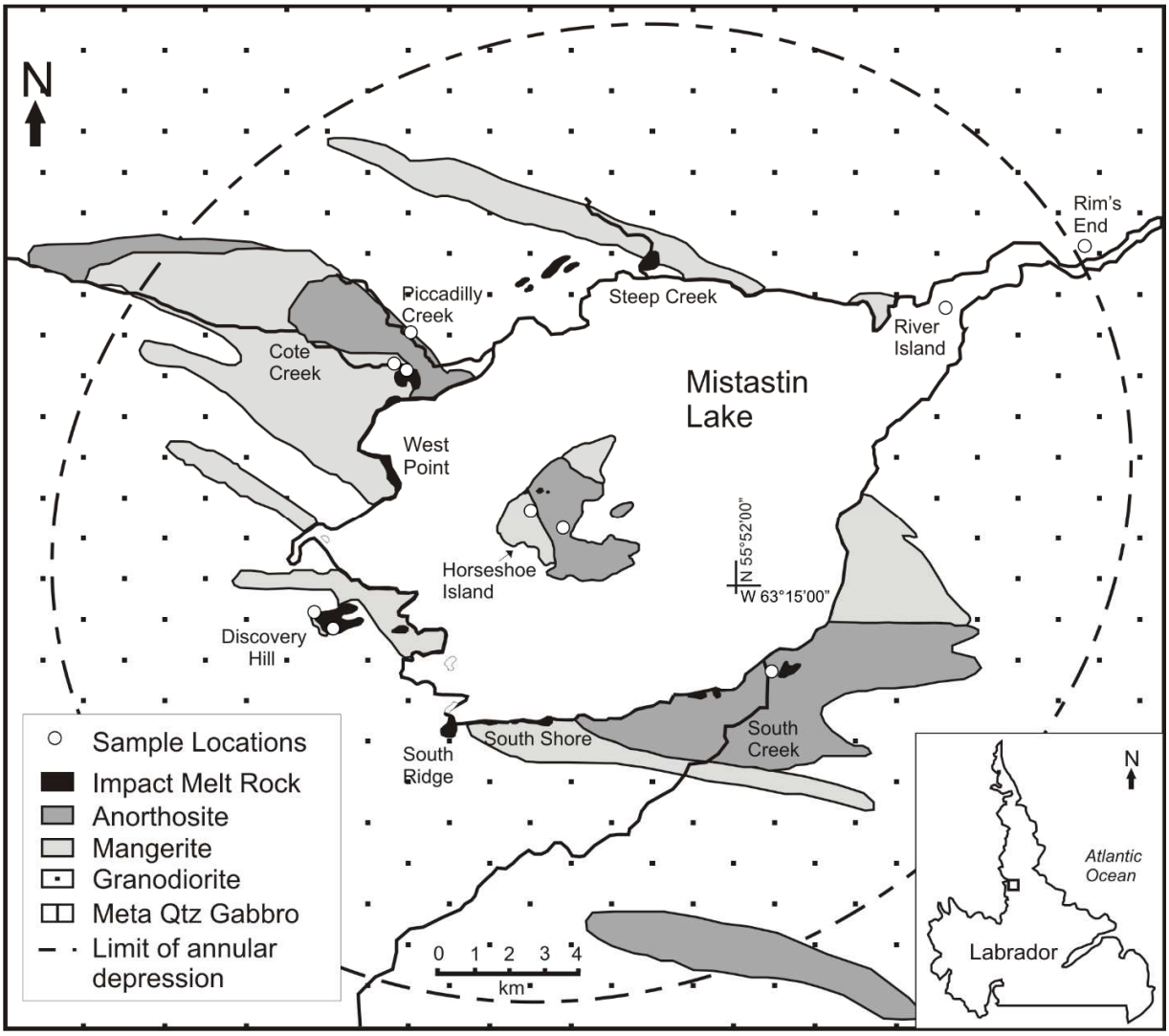

Fig. 1. A simplified geological map of the Mistastin Lake impact structure showing the three main target lithologies (anorthosite, granodiorite, and mangerite). The dashed line indicates the apparent crater rim according to Grieve (1975). Samples for this study were taken from various locations and lithologies around the crater as indicated by white dots; for simplicity, samples from the same area are grouped together (i.e., the number of dots is not representative of the number of samples). Geographic locations referred to in the rest of this paper are labelled and correlate with those in Table 2. Modified from Marion and Sylvester (2010).

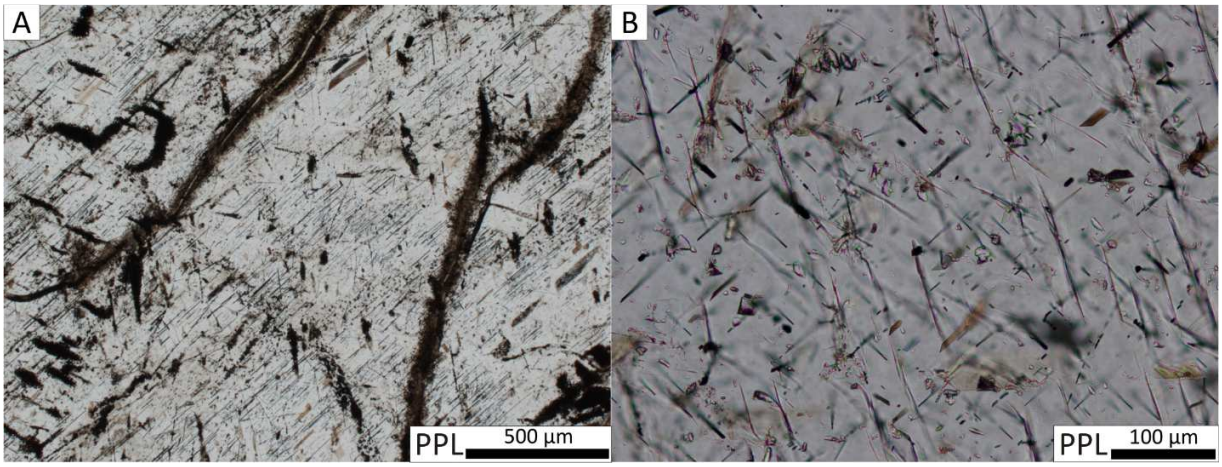

Fig. 2. Transmitted light photomicrographs of ubiquitous Fe-oxide microlites, which pervade diaplectic plagioclase glass (A) and plagioclase crystals (B) in anorthosite samples. They appear to be aligned with crystallographic planes. When viewed at low magnification (A), they may initially be mistaken for planar deformation features but at higher magnification (B) their acicular habit and discontinuity throughout the grain becomes apparent. PPL=Plane-polarized light.

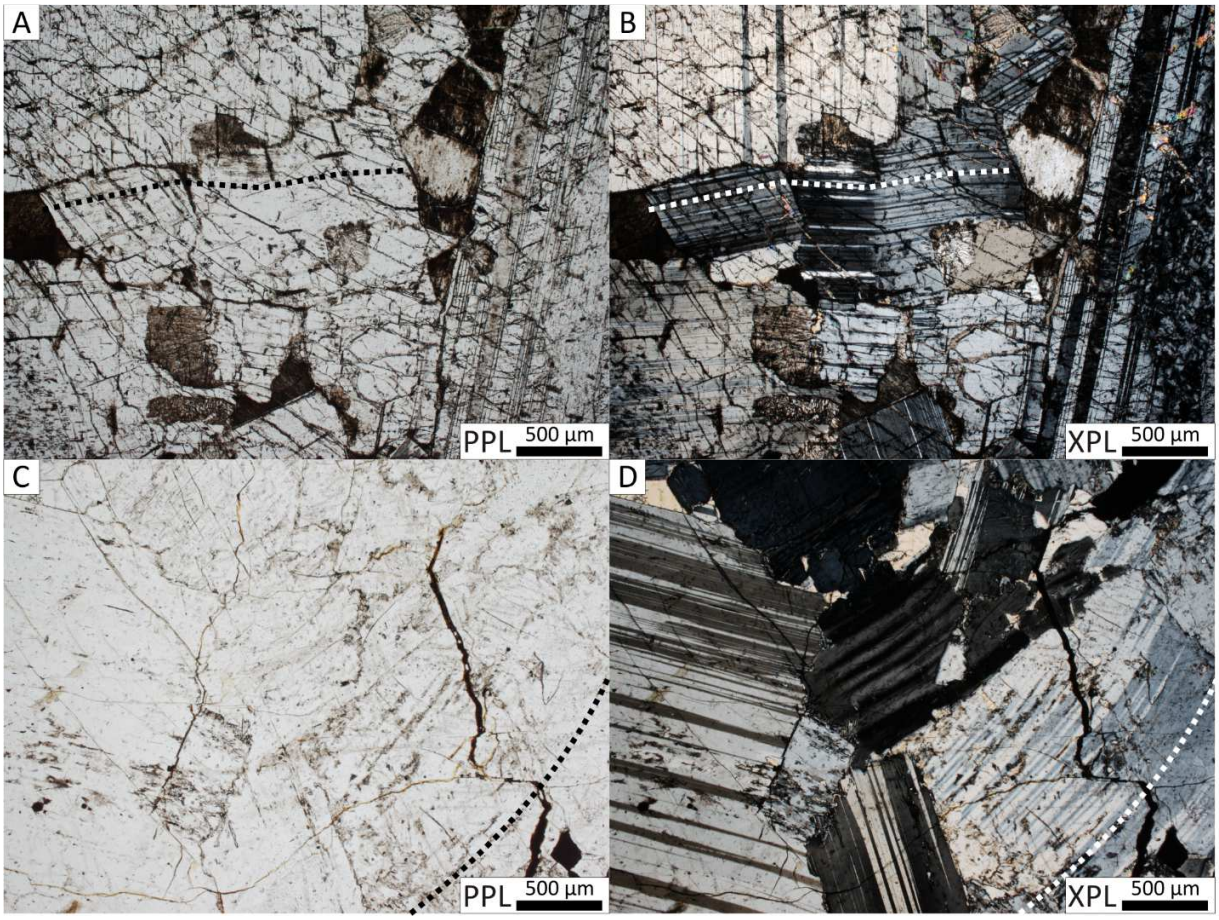

Fig. 3. Transmitted light photomicrographs of kinked and bent plagioclase twins. A, B) Kinked twins in plagioclase show optical evidence of non-uniform strain. Sharp kinks in the twins are indicated by the dotted line. The different thirds of the crystal go extinct at different times, though fairly uniformly in each section. C, D) Curved twins, indicated by the dotted line, showing a smoother bend in the crystal than the kinked twins. PPL=Plane-polarized light; XPL=Cross-polarized light.

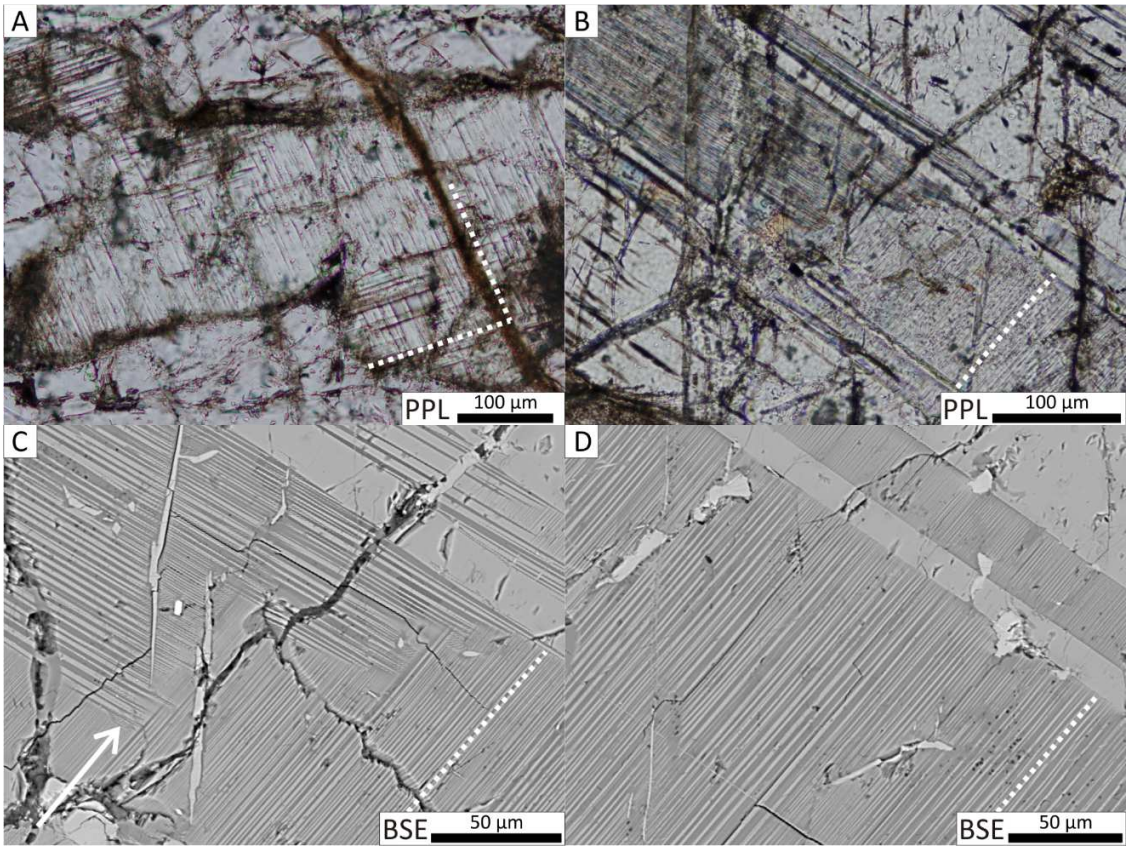

Fig. 4. Photomicrographs of PDFs in quartz, and planar features in alternate plagioclase twins. A) Transmitted light photomicrograph of PDFs in quartz from the central uplift. B) Transmitted light photomicrograph of planar features in alternate twins of plagioclase, which superficially resemble PDFs. C, D) BSE images showing compositional difference and pinching out (arrow), behavior which PDFs would not demonstrate. PPL=Plane-polarized light; XPL=Cross-polarized light; BSE=Backscatter electron image.

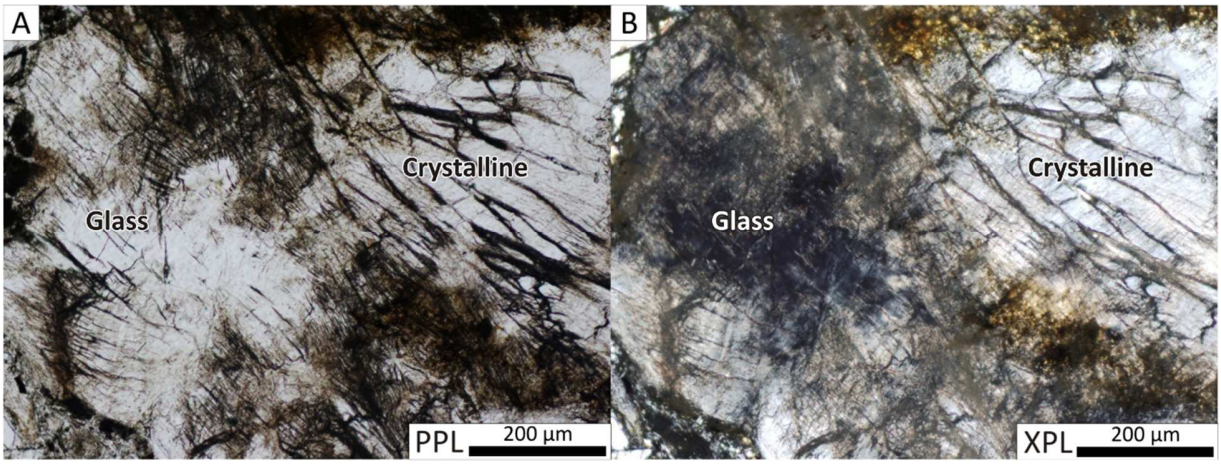

Fig. 5. Transmitted light photomicrographs of a plagioclase grain showing partial isotropization of feldspar (part of the crystal has been converted to diaplectic feldspar glass). In this case, the area that has become isotropic does not appear to be crystallographically controlled. A) The grain appears clear and transparent with significant fracturing in plane polarized light. B) A portion of the grain is isotropic (glass), remaining extinct on rotation under XPL (left, labeled 'Glass'), while the crystalline portion remains birefringent (not glass) in cross-polarized light (right, labeled 'Crystalline'). PPL=Plane-polarized light; XPL=Cross-polarized light.

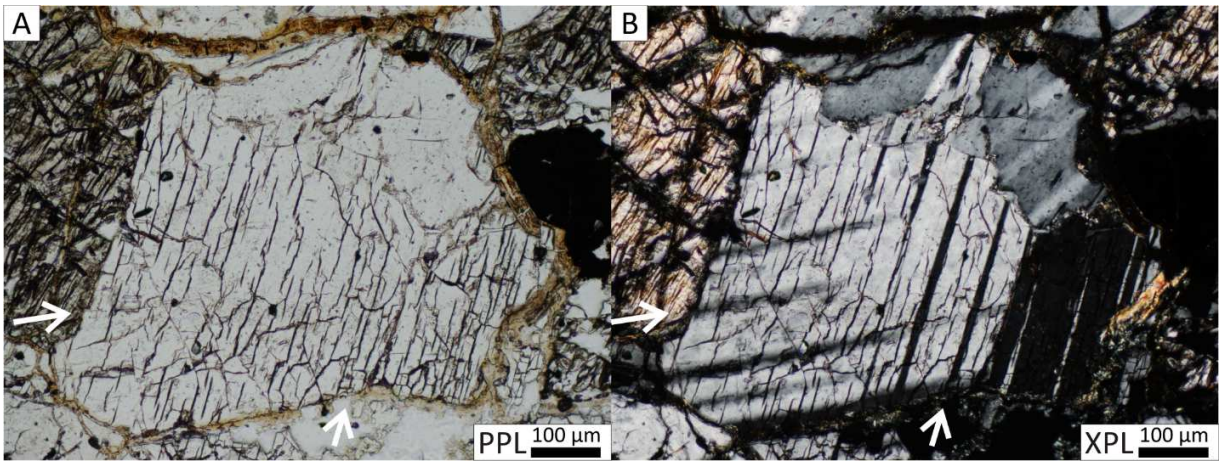

Fig. 6. A, B) Transmitted light photomicrographs of a plagioclase grain displaying alternate twin isotropization (two sets of twins that have been converted to diaplectic glass). In (B) the sets of twins that are black remain extinct on rotation of the stage. PPL=Plane-polarized light; XPL=Cross-polarized light.

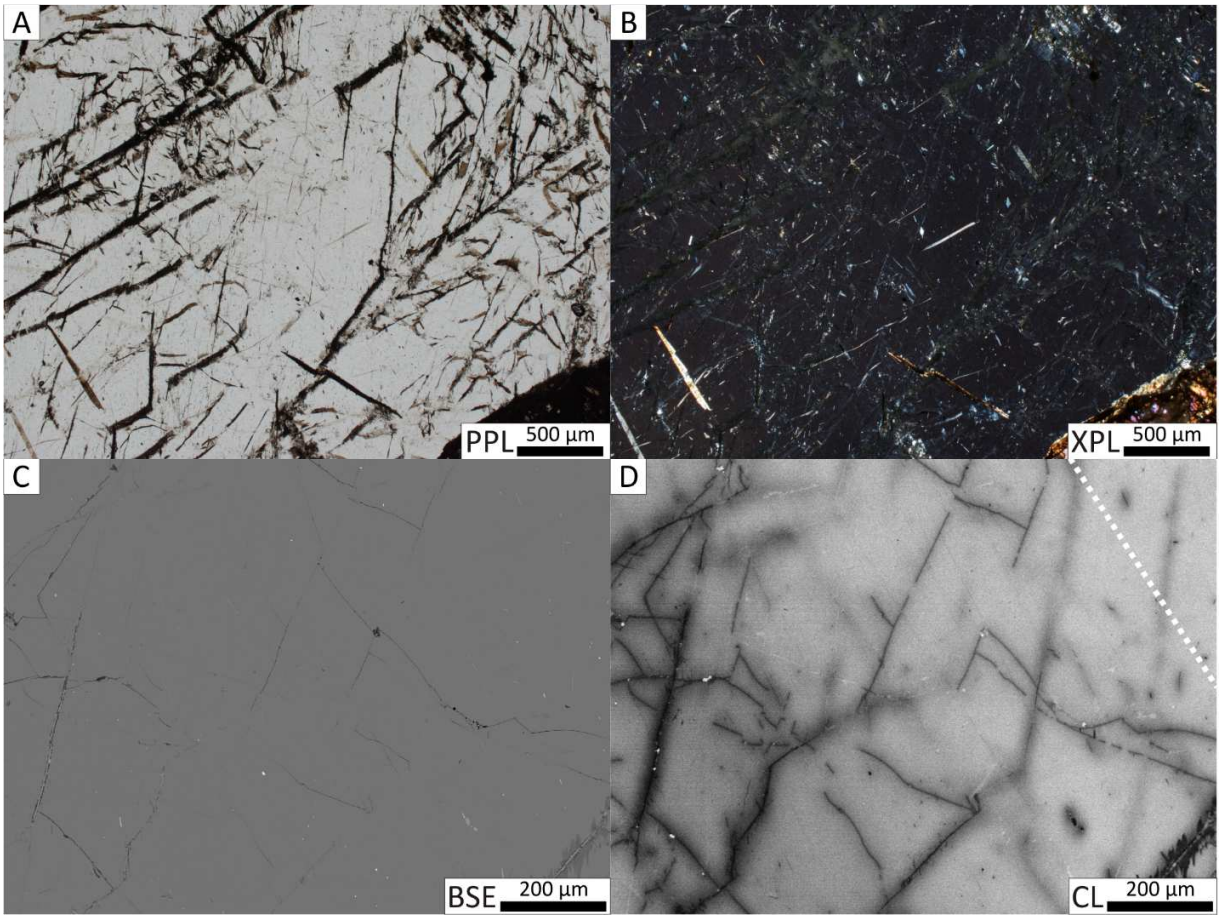

Fig. 7. Transmitted light photomicrographs (A, B), a BSE image (C), and a CL image (D) of diaplectic plagioclase glass. A, B) Except for inclusions the grain remains extinct on rotation of the stage under crossed polarized light. C) No linear features are apparent in BSE images. D) There are some linear features apparent in CL that are aligned with the dotted line that might be relict evidence of twins. PPL=Plane-polarized light; XPL=Cross-polarized light; BSE=Back-scatter electron image; CL=Cathodoluminescence image.

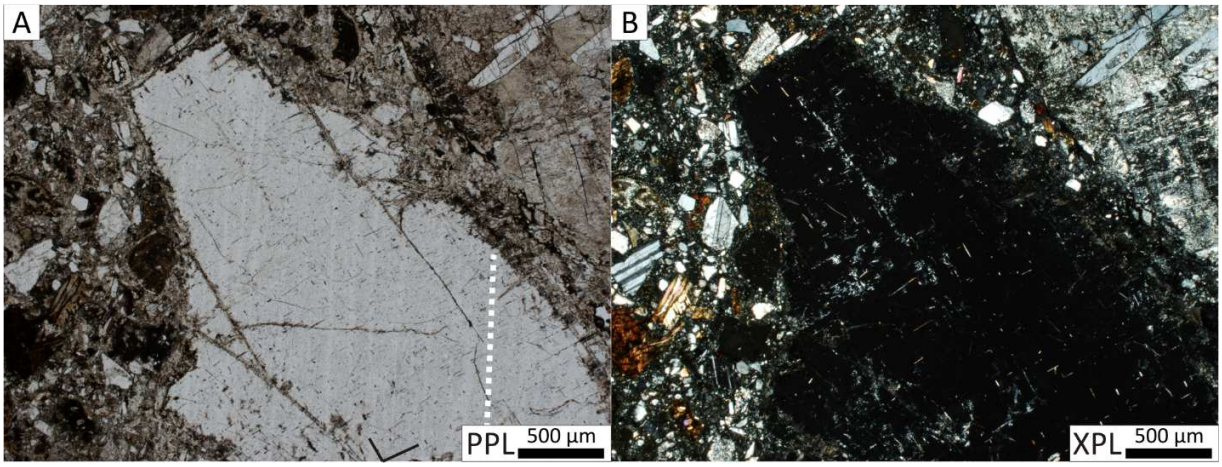

Fig. 8. Transmitted light photomicrographs of a diaplectic plagioclase glass clast in a lithic impact breccia. A) PPL shows lamellae aligned with the dotted line. They appear to show remnant structure within the glass. There is no evidence of these in either XPL (B), BSE (not shown), or CL (not shown). PPL=Plane-polarized light; XPL=Cross-polarized light.

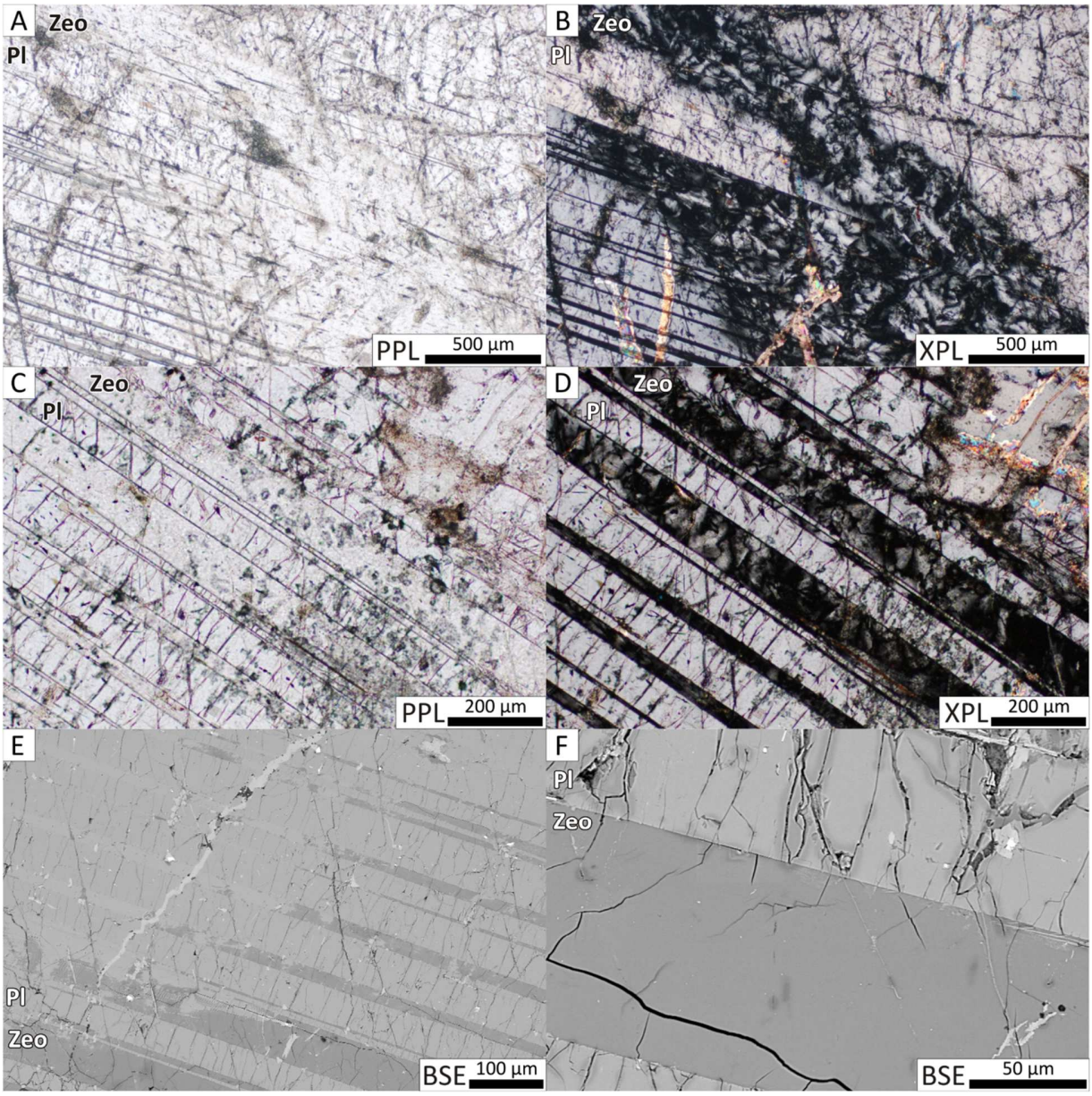

Fig. 9. Transmitted light photomicrographs (A–D) and backscattered electron (BSE) images (E, F) of the zeolite phase levyne-Ca, which appears pseudomorphous to the surrounding plagioclase in both transmitted light (A-D) and BSE (E, F). Note that in PPL (A, C) the zeolitized area is clear and has fewer fractures than the surrounding plagioclase. A, B) zeolitization which appears vein like; on the right side of the image it crosses a crystal boundary, while on the left it is abruptly halted by the same. C, D) Preferential zeolitization of alternate twin lamellae. Note the perpendicular fractures in the neighbouring plagioclase twins, which do not exist in the zeolitized twins. E-F) BSE images of the alternate zeolite twins showing compositional difference and highlighting the fractures, which are truncated by the zeolite. PPL=Plane polarized light; XPL=Cross-polarized light; BSE=Back-scatter electron image. Pl=plagioclase; Zeo=zeolite.

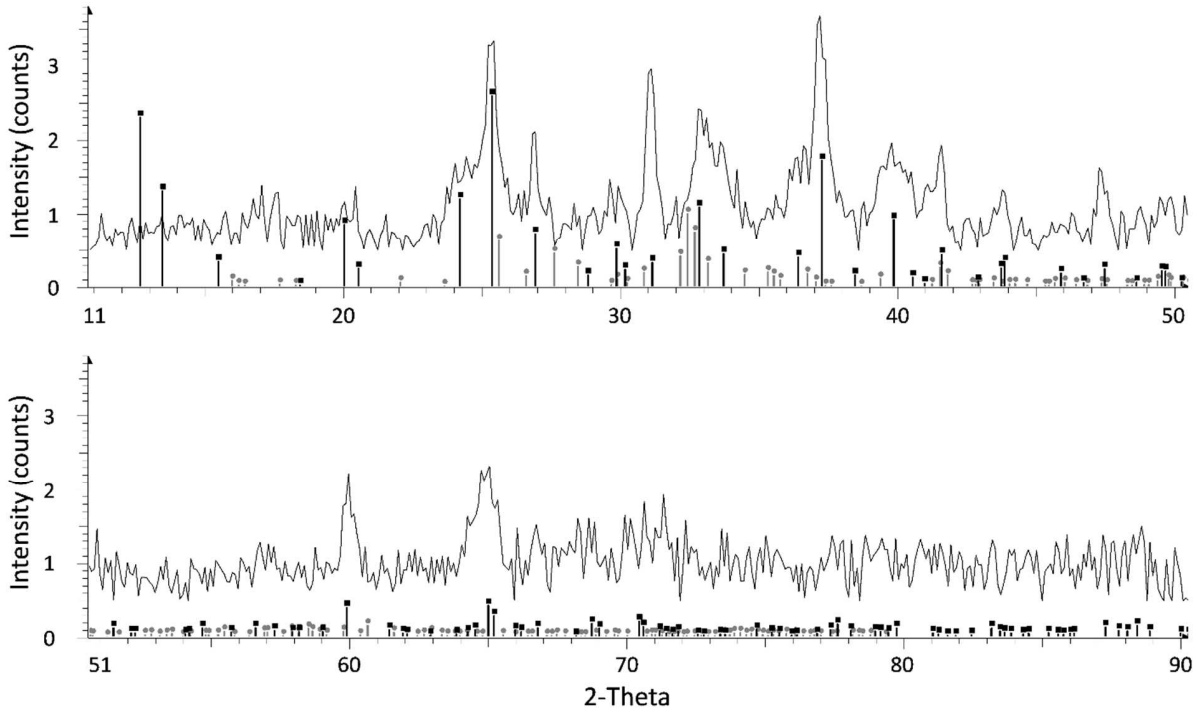

Fig. 10. µXRD plot of intensity versus 2θ for the alteration pictured in Figure 9B. The pattern matches the zeolite levyne-Ca (ICDD card 00-046-1263(C)) (black sticks topped with squares). The grey sticks (topped with circles) are the closest plagioclase match, andesine (ICDD card 01-079-1148 (C)), shown here to demonstrate that the measured pattern matches levyne-Ca more than andesine.

TABLES

Table 1. A summary of shock effects in plagioclase feldspar according to the three main existing schemes.

Stöffler (1971)			Stöffler et al. (1991)			Singleton et al. (2011)		
Shock stage	Shock effects	Pressure (GPa)	Shock stage	Shock effects	Pressure (GPa)	Shock level	Shock effects	Pressure (GPa)
0	Fractured		*S1* Unshocked	Sharp optical extinction, irregular fractures	<4-5	0		0
						1		2-5
			S2 Very weakly shocked	Undulose extinction, irregular fractures		2	Fracturing checkerboard	5-10
I	Diaplectic feldspar (shocked, but not yet amorphous)	10	*S3* Weakly shocked	Undulose extinction	5-10	3	PDFs, checkerboard	10-20
			S4 Moderately shocked	Undulose extinction, partially isotropic, PDFs	15-20		PDFs, reduced refractive index, lower birefringence, checkerboard	20-30
						4	PDFs	30-35
II	Diaplectic feldspar glass	35	*S5* Strongly shocked	Maskelynite	30-35	5	Diaplectic to flowed and vesicular, partial melting, normal (melted) glass	35-45
							Diaplectic to flowed and vesicular, partial melting	45-55
III	Fused feldspar (vesiculated glass)	45	*S6* Very strongly shocked	Shock melted (normal glass) restricted to local regions in or near melt zones	45-55	6	Flowed to frothy glass, partial melting	55-60
IV	Inhomogeneous rock glasses	55-60				7	Complete melting of all minerals, frothy siliceous, and minor mafic glasses	60-80
V	Silicate vapour	>80	Shock melted	Whole rock melting	75-90	8	Complete rock vaporization	>80

Stöffler (1971) and Singleton et al. (2011) are based on studies of terrestrial shocked rocks. Stöffler et al. (1991) is based on classification of ordinary chondrites.

Table 2. Geographic distribution of Mistastin samples and their optical characteristics.

Crater location	**Geographic location***	**Sample Name** (individual samples separated by semi-colon)	**Rock type**	**Optical effects**							
				Offset twins	Fractures	Undulose extinction	Bent twins	PDFs (quartz)	Levyne-Ca	Diaplectic feldspar glass (partial**)	Diaplectic feldspar glass (complete)
Central uplift	Horseshoe Island	***MHI10:*** 04; 12; 17; 22; 23; 35; 51; 54; 54-2 ***MST09:*** 20; 22; 24; 25; 26	Anorthosite	x	x	x	x	x	x		
Inner terrace	Coté Creek	***MM09:*** 35A, 35D, 35E	Clast rich melt		x	x					
		MM10: 05-B1; 05-B2; 05-C; 06-A2; 06-A3; 06-D2; 09-B; 10; 11; 12-2; 13-1; 13-2; 16; 17-A; 17-B; 34-A; 34-C2; 34-C5	Polymict (mostly anorthosite) lithic breccia		x	x	x			x	x
			Polymict lithic breccia		x						x
	Piccadilly Creek	***MM10:*** 20; 20-1; 20-2; 24; 25; 28; 30; 32	Monomict anorthosite breccia	x	x	x					
	South Creek	***MM10:*** 36-B1; 36-B2; 38; 39; 40; 41-1; 42; 43; 44; 45; 46-2	Monomict anorthosite breccia		x	x	x		x		x
Inner terrace/melt pond	Discovery Hill	***MM10:*** 01-C	Polymict glass-bearing breccia		x	x					
Inner Terrace	Steep Creek	***MM09:*** 10; 32-B	Polymict glass-bearing breccia		x	x		x		x	x
Outer Terrace Rim	River Island	***MM10:*** 32-A; 32-B; 33	Mangerite		x	x					
			Granodiorite		x	x					
	Rim's End	***MM10:*** 47; 48	Mangerite		x						

*These locations are indicated in Figure 1.

**Including alternate twin isotropization.

Crater location elaborated on by Mader and Osinski (2011), Mader et al. (2013). Rock type classification elaborated on by Mader and Osinski (2013).

Table 3. Average composition of plagioclase feldspars, levyne-Ca, diaplectic feldspar glasses, and alkali feldspars.

Phase	Feldspar		Feldspar		Feldspar		Feldspar		Feldspar**		Levyne-Ca	
Sample #	MM10-011		MM10-048		MM10-032b		MM10-040		MHI10-17		MHI10-17	
Grain count	5		3		1		9		5		3	
Rock Type	Anorthosite breccia		Granodiorite		Mangerite		Anorthosite Breccia		Anorthosite		Anorthosite	
Location	Coté Creek 1		Rim's End		River Island		South Creek		Central Uplift		Central Uplift	
# of analyses	24		15		5		45		20		12	
An content	An_{47}		An_{31}		An_{31}		An_{49}		An_{55}		N/A	
	wt %	s.d.	wt %	s.d.	wt %	s.d.	wt %	s.d.	wt %	s.d.	wt %	s.d.
SiO_2	56.73	1.07	60.89	0.29	60.94	0.49	56.29	0.56	54.59	0.57	47.85	0.75
Na_2O	5.80	0.36	7.75	0.08	7.79	0.32	5.48	0.20	5.39	0.16	0.27	0.05
Al_2O_3	27.43	0.57	25.17	0.17	25.37	0.56	28.36	0.35	27.82	0.40	22.89	0.41
K_2O	0.47	0.09	0.34	0.03	0.21	0.05	0.37	0.07	0.40	0.02	0.63	0.06
CaO	9.07	0.59	6.11	0.17	6.17	0.43	10.00	0.40	10.03	0.43	11.02	0.09
Total	99.90	0.87	100.45	0.44	100.67	0.27	100.92	0.58	98.22	0.35	82.67	1.18
Cations												
SiO_2	7.65	0.10	8.09	0.02	8.07	0.07	7.53	0.05	7.50	0.07	7.73	0.03
Na_2O	1.52	0.09	2.00	0.02	2.00	0.08	1.42	0.05	1.44	0.04	0.09	0.01
Al_2O_3	4.36	0.11	3.94	0.02	3.96	0.08	4.47	0.05	4.51	0.07	4.36	0.03
K_2O	0.08	0.02	0.06	0.00	0.04	0.01	0.06	0.01	0.07	0.00	0.13	0.01
CaO	1.31	0.09	0.87	0.02	0.88	0.06	1.43	0.06	1.48	0.06	1.91	0.03
Total	14.96	0.02	14.97	0.01	14.97	0.02	14.97	0.02	15.00	0.02	14.20	0.02

*Abbreviations: wt% = mean composition in weight%; s.d. = standard deviation

**These feldspars are from parts of the crystal adjacent to the zeolite levyne-Ca

(Table 3 continued)

Phase	Diaplectic Glass		Diaplectic Glass		Diaplectic Glass		Diaplectic Glass		K-Feldspar		K-Feldspar	
Sample #	MM10-34C-5		MM10-38		MM09-035D		MM10-13-2		MM10-048		MM10-032b	
Grain count	3		8		5		8		3		2	
Rock Type	Polymict Breccia		Anorthosite Breccia		Anorthosite		Anorthosite		Granodiorite		Mangerite	
Location	Coté Creek		South Creek		Coté Creek		Coté Creek		Rim's End		River Island	
# of analyses	15		40		25		40		13		8	
An content	N/A		An_{44}		An_{47}		An_{50}		N/A		N/A	
	wt %	s.d.	wt %	s.d.	wt %	s.d.	wt %	s.d.	wt %	s.d.	wt %	s.d.
SiO_2	46.40	2.04	56.17	0.81	54.85	0.74	55.94	0.63	65.35	0.85	64.97	0.48
Na_2O	3.81	1.30	3.14	0.48	3.26	0.46	3.16	0.46	2.13	1.31	1.85	1.29
Al_2O_3	22.57	4.09	28.19	0.82	28.19	0.49	29.17	0.38	19.53	0.43	19.48	0.42
K_2O	0.50	0.45	0.48	0.04	0.61	0.10	0.41	0.04	13.22	2.42	13.61	2.25
CaO	6.75	1.00	9.59	0.56	9.38	0.50	10.30	0.40	n.d.	0.30	n.d.	0.31
Total	80.26	6.69	97.94	1.01	96.71	1.15	99.31	0.40	100.21	0.52	100.30	0.19
Cations												
SiO_2	7.76	0.42	7.65	0.11	7.59	0.07	7.54	0.07	8.95	0.02	8.94	0.03
Na_2O	1.23	0.39	0.83	0.13	0.87	0.13	0.83	0.12	0.56	0.34	0.49	0.34
Al_2O_3	4.39	0.54	4.53	0.10	4.60	0.06	4.63	0.06	3.15	0.03	3.16	0.04
K_2O	0.11	0.10	0.08	0.01	0.11	0.02	0.07	0.01	2.32	0.45	2.39	0.41
CaO	1.20	0.14	1.40	0.08	1.39	0.06	1.49	0.06	n.d.	0.04	n.d.	0.05
Total	14.72	0.29	14.53	0.11	14.60	0.10	14.59	0.10	14.91	0.08	14.92	0.03

*Abbreviations: wt% = mean composition in weight%; s.d. = standard deviation; n.d. = not detected

**These feldspars are from parts of the crystal adjacent to the zeolite levyne-Ca